Chemical Science

ROYAL SOCIETY OF CHEMISTRY

REVIEW

View Article Online
View Journal | View Issue

Cite this: *Chem. Sci.*, 2025, **16**, 12702

Organic mechanoluminescent nanoparticles for biomedical applications

Christina Gu,†[a] Xiangping Liu,†[a] Brian Song,[b] Wenliang Wang,[a] Weilong He[a] and Huiliang Wang *[a]

Mechanoluminescence has emerged as a promising tool for biomedical applications, particularly when paired with ultrasound to enable remote activation. These mechanoluminescent systems have shown potential by offering non-electrical, remote control over biological processes, particularly in fields of neuromodulation and bioimaging. Among these systems, organic mechanoluminescent nanoparticles have garnered attention for their biocompatibility, structural flexibility, light weight properties, and biodegradability, positioning them as ideal candidates for next-generation biomedical devices. This review summarizes recent progress on new designs, discoveries, and mechanisms in the research of organic mechanoluminescent materials, with a focus on their innovative applications in neuromodulation, bioimaging and theranostics; meanwhile also exploring their potential in optophysiology and other biomedical applications. By highlighting the advances of organic mechanoluminescent systems, this review underscores their transformative potential in enabling novel light-mediated bioapplications.

Received 4th April 2025
Accepted 22nd June 2025

DOI: 10.1039/d5sc02526e

rsc.li/chemical-science

1 Introduction

Mechanoluminescence (ML) is the phenomenon of light emission from specific mechanoluminescent materials triggered by mechanical stimulation such as grinding, crushing, or pressing.[1] The discovery of this phenomenon dates to 1605 when Francis Bacon discovered light production upon scraping a sugar cube with a knife.[2] Centuries later, ML is reported from a variety of substances: solid compounds such as quartz and ruby, semiconducting polymers, inorganic nanoparticles, and organic nanoparticles.[3] The scientific exploration of ML gained significant momentum in the recent centuries as researchers sought to understand its fundamental mechanisms and potential applications. An attractive aspect of ML is its capability of indicating mechanical force as light sources within biological and physiological environments. Since then, many mechanoluminescence mechanisms using various materials have been introduced.

ML in solids can be broadly classified into two main categories based on its mechanism: mechanofluorochromic luminescence and triboluminescence.[4] Some materials exhibit both mechanofluorochromism and triboluminescence, depending on the stress applied and their molecular structure. Another approach differentiating ML considers the mechanical nature of the applied stress: fractoluminescence, plasticoluminescence, and elasticoluminescence.[5] Elasticoluminescence stands out among these mechanisms for their nondestructive nature. The development of nondestructive ML materials has been a crucial advancement in the field, allowing for repeated light emission without material degradation. A common theory for ML emission is the piezoelectric effect, which is typically implemented using noncentrosymmetric compounds. Meanwhile, centrosymmetric compounds were found to produce luminescence due to reactions such as cycloreversion.[6] Since then, piezoelectric effect, crystal structure disorder and conformation transitions have been implemented to enable dynamic luminescence responses in a variety of solids.[7–9] These traditional ML mechanisms are typically used for stress sensing and detection, lighting and display technologies, and optical signaling and illumination.[10–12] In general, the versatility and tunability of ML materials present a wide range of applications.

A key discovery in ML is the development of mechanoluminescent nanoparticles (MLNPs). The first application of MLNPs in the biomedical field was in 1999 by Xu *et al.*, who used $SrAl_2O_4$:Eu^{2+} nanoparticles to illuminate stress distribution in hard tissue upon excitation using direct servohydraulic pressure.[13] Currently, MLNPs stand out for their ability to be excited by hydrodynamic pressure rather than the bulk static stress of traditional ML, greatly expanding the application of ML *in vitro* and *in vivo* environments. One of the most promising applications of MLNPs for the biomedical domain is the emerging of ultrasound-induced ML. This mechanism leverages acoustic

[a]*Biomedical Engineering Cockrell School of Engineering, The University of Texas at Austin, Austin, Texas 78712, USA. E-mail: evanwang@utexas.edu*

[b]*Department of Neuroscience, The University of Texas at Austin, Austin, Texas 78712, USA*

† These authors contributed equally to this work.

waves to excite ML materials, converting mechanical energy into luminescent emission that can be used for noninvasive imaging, therapeutic interventions, neuromodulation, and even brain computer interfaces.[14–17] Unlike traditional optical methods that suffer from scattering and attenuation in biological tissues, ultrasound can penetrate deep into the body to enable precise activation of ML materials at targeted locations.[18,19] Additionally, ultrasound-based ML is noninvasive and biosafe, as it does not require ionizing radiation or high-energy lasers, minimizing potential harm to tissues.[20–22] Using ultrasound, Wu *et al.* first developed inorganic MLNPs, ZnS doped with Cu and Ag, for neuromodulation in 2019.[23] Meanwhile, other effects of ultrasound include sonochemistry, acoustic activation, reactive oxygen species (ROS) generation, and sonoluminescence, which can be coupled with ML for novel applications.[24–26] Currently, ultrasound-induced MLNPs have been implemented in biosensing, bioimaging, and neuromodulation, and are being explored for their potential in therapeutic interventions. The ability to remotely trigger light emission within biological tissues enables precise control over neural activity, paving the way for noninvasive neuromodulation techniques. Ultrasound induced ML provides high-resolution bioimaging capabilities by providing localized light sources that enhance contrast and depth penetration, while the controlled dispersion of light within tissues can facilitate therapeutic applications.

A clear distinction between ML and the more commonly photoluminescence (PL) is that it does not require external light excitation, as it is able to directly convert mechanical force to light. This makes it advantageous for *in vivo* biomedical applications as it can enable deep-tissue imaging and real-time stress sensing with minimal background noise. Additionally, ML-based nanoparticles are more biocompatible for long-term use since they eliminate risks associated with UV/visible light exposure, such as DNA damage, tissue autofluorescence, photodamage, and limited penetration depth.[27] These advantages make ML ideal for biomedical applications.

An exciting frontier in MLNP research is the development of organic mechanoluminescent nanoparticles, which are typically activated by ultrasound stimulation. Organic MLNPs offer several advantages over their inorganic counterparts, specifically in their biocompatibility and biodegradability for *in vivo* environments.[28] The use of organic MLNPs will overcome clinical safety concerns posed by inorganic ML and currently invasive processes. Organic MLNPs feature highly adjustable chemical structures, allowing for tunable emission properties and enabling the development of colorful emission profiles, expanding their usability in optogenetics and bioimaging technologies.[29] Furthermore, the lightweight and solution-processable nature of organic MLNPs makes them highly desirable. Organic MLNPs open new avenues for deep tissue imaging, remote modulation of cellular and molecular functions, and novel therapeutic interventions.[23] As research continues to advance, the integration of ML materials into biomedical technologies is expected to revolutionize noninvasive diagnostics and treatment strategies, solidifying ML as a cornerstone of future biomedical innovation.

Currently, the field of organic MLNPs in biomedical applications remains relatively underexplored with only a few confirmed applications due to its novelty and rarity. This review offers insight into recent advancements in the research and implementation of organic MLNPs with a focus on ultrasound emission mechanisms in fields such as neuromodulation, bioimaging, and other prospective biomedical applications.

2 Organic mechanoluminescent nanoparticles

Organic MLNPs have garnered significant attention and breakthroughs in recent years for their strong potential applications in bioimaging, deep brain neuromodulation, and therapeutic monitoring. Many compositions and designs of organic MLNPs have been put forward. The luminescent behavior of these materials is highly correlated with their configuration and intermolecular state, and their emission mechanisms are primarily driven by hydrodynamic stimuli, specifically ultrasound. This section will explore the composition and mechanisms of organic MLNPs.

2.1 The composition of organic mechanoluminescent nanoparticles

Traditional organic compound-based ML materials rely on organic luminophores, which undergo conformational changes under mechanical stress, enabling light emission. Their ML behavior is closely tied to photoluminescence properties, molecular packing, spatial conformation, and intermolecular interactions.[30] These luminophores are often embedded in matrices or nanoparticles to enhance energy transfer and emission efficiency. Advanced strategies such as isostructural doping, substitution, and heterojunction formation further improve performance. Organic ML materials include conjugated polymers, small organic molecules, and fluorescent dyes, with notable examples like carbazole, phenothiazine, and tetraphenylethene derivatives.[31–33] Most exhibit mechanofluorescence with fast singlet-state emission, while rarer mechanophosphorescent materials provide long-lived emission desirable for sensing applications. To design these materials, Huang *et al.* proposed the Molecular Uniting Set Identified Characteristic (MUSIC) framework to connect molecular packing motifs with solid-state luminescent responses.[34] This framework categorizes materials by how mechanical stress triggers specific emission mechanisms, such as excimer formation, defect emission, or piezochromic luminescence, providing predictive guidelines for developing tailored organic ML systems.

Thus, most mechanoluminescent materials reported have been bulk solids, with fractal or deformity-based ML emission mechanisms. More recently, researchers have moved toward the development of ML fluids through the suppressed dissolution of MLNPs.[35] ML liquids are easily delivered through a flow system and *in vivo* as opposed to bulk solids. Additionally, mechanoluminescence was chosen as it's a much more efficient and safer way to convert mechanical energy into light,

compared to other techniques such as sonoluminescence. ML fluids were first developed by Hong *et al.* using $Sr_2MgSi_2O_7$:Eu,Dy, ZnS:Cu,Al, ZnS:Mn, and $CaTiO_3$:Pr to create stable aqueous solutions that span from 470 nm to 610 nm emission spectra under ultrasound stimulation. The high performance of ZnS and Sr has inspired the search for more MLNPs, especially those with elastic ML that can achieve repeatable luminescence. The most popular method is utilizing piezoelectric host materials such as quaternary oxysulfides, oxonitridosilicates, and niobates doped with lanthanide and other metal ions.[36–39]

Parallel to the development of inorganic nanoparticles are that of their organic counterparts, which are typically more advantageous in bioapplications due to their biocompatibility. In 2022, Pu *et al.* introduced organic MLNPs named SNAPs, that exhibited afterglow luminescence after ultrasound stimulation (Fig. 1a).[40] SNAP is the combination of a sonosensitizer and a substrate with agents that generate singlet oxygen ($^1O_2$) upon ultrasound excitation and emit visible to NIR range light. Meanwhile, small molecules that react with ROS to produce self-luminescence dioxetane intermediates were chosen as substrates. Through the co-precipitation of a sonosensitizer and a substrate with PEG-*b*-PPG-*b*-PEG, SNAPS were produced and tested for luminescence intensity and wavelength under ultrasound excitation. It was found that the NCBS sonosensitizer and azide–methyl acrylate–phenoxyl–adamantylidene substrate had the highest sonoafterglow among other combinations tested, with peak at 500 nm. The group found that the use of ultrasound-induced sonoafterglow overcomes the issues of light absorption faced by photoluminescent approaches. As a result,

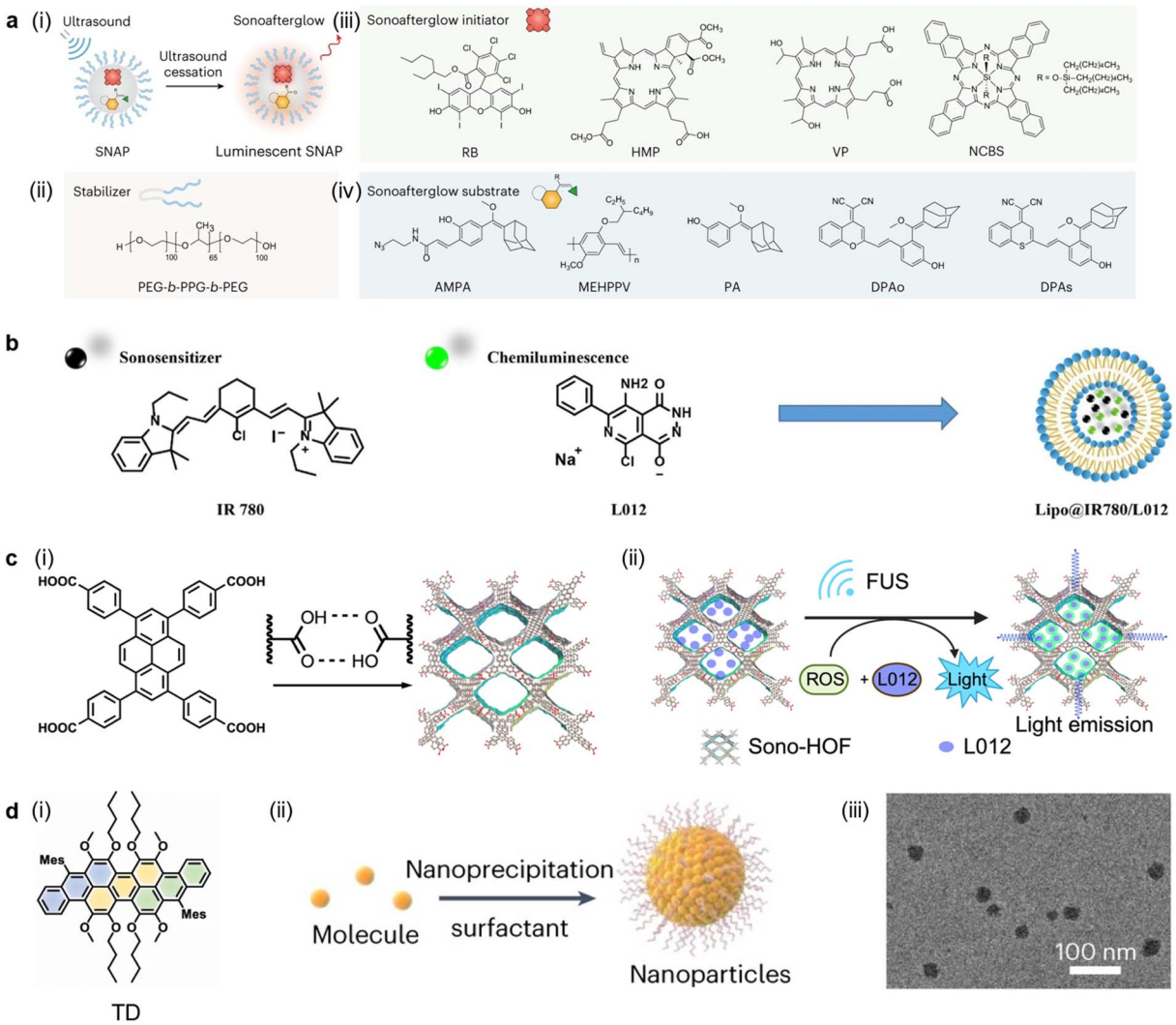

Fig. 1 The composition of different types of organic mechanoluminescent nanoparticles. (a) Schematic of sonoafterglow illustration (i) alongside the components of SNAPs, which include sonoafterglow stabilizers (ii), initiators (iii), and substrates (iv). Reproduced with permission from ref. 40. Copyright 2023, Springer Nature. (b) Schematic illustration of liposome formulation loaded with IR780 (sonosensitizer) and L012 (chemiluminescence molecule) to form Lipo@IR780L012. Reproduced with permission from ref. 28. Copyright 2023, American Chemical Society. (c) Schematic of preparation of sonosensitized HOF nanoparticles (i) and ultrasound cascade in HOF nanoparticles (ii). Reproduced with permission from our previous work ref. 42. Copyright 2025. (d) Chemical structure of TD molecule (i); schematic illustration of nanoparticle preparation (ii); TEM image of TD NPs (iii). Reproduced with permission from ref. 44. Copyright 2024, Springer Nature.

the sonoafterglow of the SNAP was found to have 2.7 times higher intensity than that of photoafterglow nanoparticles.

In 2023, Wang *et al.* developed liposome based organic nanoparticle light sources for noninvasive deep brain sono-optogenetic stimulation (Fig. 1b).[28] A single layer of lamella was used to create a unilamellar vesicle. The vesicle was loaded with the sonosensitizer IR780 and the chemiluminescent L012, for a complete structure named Lipo@IR780/L012. Upon ultrasound excitation, IR780 generates ROS which activates L012 to produce light. The Lipo@IR780/L012 structure was found to be extremely stable with minimal changes or leakage. The advantage of the unilamellar vesicle was its small size of 120 nm, its biocompatibility as a lipid, and its ability to easily travel through the bloodstream and circumvent rapid clearance *via* the reticuloendothelial system, liver, and kidney after intravenous injection. Luminescence testing using Lipo@IR780/L012 revealed its capability of repeated visible blue light emission for over 90 s of ultrasound irradiation. Increasing the mechanoluminescence intensity is still crucial especially for deep-brain neuromodulation. They doped CaO_2 into the original system and fabricated new MLNPs named Lipo@IR780/L012/CaO_2, which enlarge the ROS generation, luminescence intensity, and eventually depth, successfully induced mouse ventral tegmental area (VTA) stimulation with the subsequent lever press test.[41] In 2025, Wang *et al.* reported the development of sono-optogenetic stimulation using sonosensitized hydrogen-bonded organic framework (HOF) nanoparticles that did not require the structure of a liposome and redundant sonosensitizer IR780.[42] HOF is assembled through intermolecular multivalent hydrogen bonds and π–π stacking interactions of organic building units and is promising for its porousness, uniformity, and programmability (Fig. 1c).[43] The HOF is able to act as a sonosensitizer and loads L012, producing light upon ultrasound stimulation. The high porosity of the HOF nanoparticles enables efficient L012 loading and high ROS production, producing sustained and intense luminescence.

Tan's group developed organic mechanoluminescent nanoparticles by nanoprecipitation of luminescent molecules using a surfactant to convert them into water-soluble nanoparticles (Fig. 1d).[44] The group found that of these luminescent particles, trianthracene-derivative nanoparticles (TD NPs) demonstrated the strongest luminescence intensity in both delayed and real-time luminescence in response to ultrasound upon coating with the DSPE-PEG surfactant. TD NPs luminescence intensity was 2000 times that of H_2O and over 70 times stronger than that of other nanoparticles tested. Additionally, it was also found that PFODBT-based and porphyrin-based nanoparticles, for instance Ce6 and F-PPIX, also had strong luminescent properties upon exposure to ultrasound stimulation. Furthermore, the doping of HBA–COOH into PFODBT NPs increased luminescence intensity by 121.4-fold as the ROS from PFODBT reacted with HBA–COOH to generate a higher chemiluminescence intensity.

2.2 Emission mechanisms of organic mechanoluminescence

In traditional mechanoluminescent materials, mechanical stimuli generate electronic excitation, often through the piezoelectric effect, which requires non-centrosymmetric crystal structures. Centrosymmetric materials, lacking this direct piezoelectric response, can still show mechanoluminescence *via* alternative mechanisms like triboelectric charge separation, defect recombination, or flexoelectric polarization.[45–48] These effects cause the excitation of electrons from the ground state (S_0) to higher singlet excited states (S_m). These excited electrons the rapidly relax to the lowest singlet excited state (S_1) through a fast internal conversion (IC). From this S_1 state, the electrons can return directly to the ground state (S_0), releasing energy in the form of fluorescence. Alternatively, some singlet electrons undergo intersystem crossing (ISC) to enter the triplet manifold (T_n), followed by fast IC to the lowest triplet state (T_1) and emit energy as phosphorescence (Fig. 2a).[49]

ML emission was traditionally induced through mechanical forces including compression tensile, shear, and fracture stress. Compression and tensile forces induce ML by altering the molecular conformation and intermolecular interactions within organic crystals. This method has been extensively studied in π-conjugated systems, where mechanical strain modifies energy levels, leading to emission.[50] However, this method is often material-specific and requires significant force to achieve measurable luminescence. Shear stress, often observed as triboluminescence, is a result of frictional forces that disrupt molecular arrangements, causing energy release in the form of light.[51] However, triboluminescence often requires continuous mechanical contact, limiting its applicability in controlled environments. Fracture-based ML occurs when mechanical breakage disrupts the molecular structure, leading to immediate charge redistribution and emission. Small-molecule organic crystals with rigid frameworks exhibit this behavior, making them useful for instantaneous stress detection and security applications.[52] However, the destructive nature of this method renders it unsuitable for applications requiring reversible or repeatable ML.

Currently, ultrasound mechanisms are typically preferred in biomedical applications due to several properties. Ultrasound-induced emissions are typically non-destructive, reversible, and offer easily controllable outputs. Additionally, they retain biomedical advantages such as noninvasiveness, deep tissue penetration, high spatiotemporal resolution, and reduced tissue damage compared to radiation.[53] There are two main types of ultrasound-induced ML emission mechanisms: ROS generation induced by ultrasonic cavitation and sonoluminescence for stimulating light emission and direct sonoluminescence emission *via* the piezoelectric effect and piezocatalysis.

In 2019, Gun *et al.* developed a mechanoluminescent mechanophore that exhibits color change under ultrasound stimulation.[54] 1,2-Dioxetane mechanophore was embedded in a synthetic elastomer such as polydimethylsiloxane (PDMS) and emits visible blue light upon mechanical activation by ultrasound (Fig. 2b). This occurs through bond scission in the dioxetane, leading to luminescence in the presence of a DPA sensitizer. The activation occurs precisely at the ultrasound focal spot, demonstrating the ability to target mechanophore activation without affecting surrounding material. Later, Liu

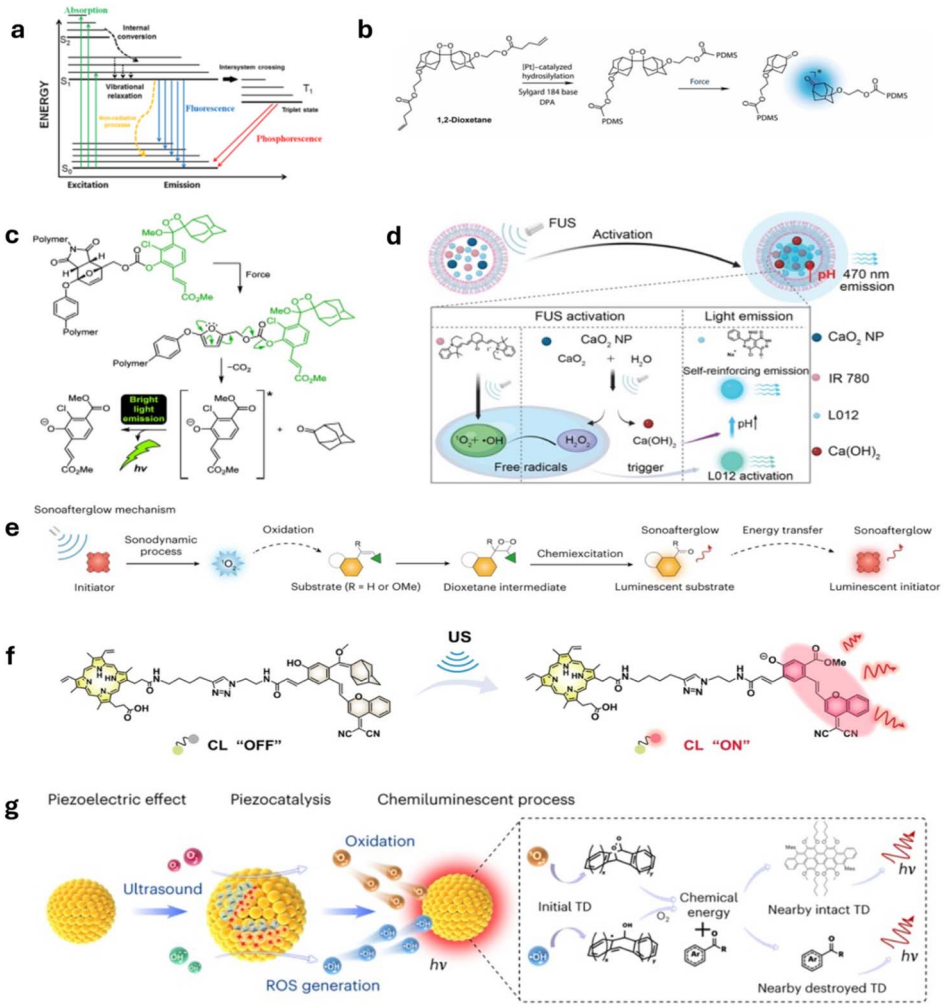

Fig. 2 The mechanisms of various organic mechanoluminescence. (a) Jablonski diagram depicting changes in energy states that lead to fluorescence. Reproduced from ref. 49. Opensource 2021, Springer Nature. (b) Schematic of 1,2 dioxetane cross-linked with PDMS mechanism for blue light emission. Reproduced with permission from ref. 54. Copyright 2019, National Academy of Sciences. (c) Schematic of 2-furylcarbinol light emission reaction mechanism. Reproduced with permission from ref. 55. Copyright 2024, American Chemical Society. Licensed under CC BY 4.0. (d) Mechanism for FUS-triggered light emission from mechanoluminescent nanoparticles. Reproduced with permission from ref. 41. Copyright 2023, American Chemical Society. (e) Schematic of sonoafterglow molecular mechanism. Reproduced with permission from ref. 40. Copyright 2023, Springer Nature. (f) Schematic of US-activated PNCL for NIR CL imaging illustration of sonoafterglow mechanism. Reproduced with permission from ref. 57. Copyright 2023, American Chemical Society. (g) Schematic diagram of TD NPs ultrasound-induced luminescence mechanism. Reproduced with permission from ref. 44. Copyright 2024, Springer Nature.

et al. developed another mechanoluminescent-mechanophore system to produce bright light emission without the use of sensitization.[55] This system consists of poly(methyl acrylate) covalently embedded with masked 2-furylcarbinol mechanophores conjugated with an adamantylidene–1,2 dioxetane chemiluminophore. Under ultrasound activation, the mechanophores trigger a reaction cascade that generates an electronically excited benzoate ester, which emits a green photon to return to its ground state (Fig. 2c).

ML emission caused by ROS generation under ultrasound stimulation is the earliest method developed for biomedical applications. Acoustic cavitation from ultrasound excitation incites the formation, growth, and violent collapse of bubbles in liquids to trigger the production of ROS. These ROS can then react with chemiluminescent molecules, leading to light emission (Fig. 2d and e).[56] Atop this basis, most organic MLNPs are created using a sonosensitizer, which when exposed to ultrasound, triggers the stronger generation of ROS chemiluminescent substrate produces light in response to the ROS production. When the sonosensitizer molecule such as IR780 or HOF is triggered by ultrasound, they generate polarization charges through the piezoelectric effect, producing a large amount of ROS. In the next step, ROS can either transfer electrons to the luminescent substrate or oxidize it. As a result of the redox process, the chemiluminescent molecule enters an excited state and relaxes back to its ground state, releasing the excess energy in the form of visible light.

Advancements in cascade amplification for organic ML have significantly improved both the intensity and efficiency of ultrasound-triggered light emission, particularly for deep-tissue

applications. Wang *et al.* designed a method that increases luminescence intensity using CaO_2 nanoparticles.[41] When ultrasound disrupts the protective polyethylene glycol (PEG) coating on CaO_2 nanoparticles, it reacts with water and generate hydrogen peroxide (H_2O_2) and calcium hydroxide ($Ca(OH)_2$). The rising pH from $Ca(OH)_2$ formation enhances the luminescent nanoparticle's emission efficiency to effectively amplify the photon yield, overcoming traditional ML systems' limitations in brightness and penetration depth. By raising pH and ROS concentration, this design achieved a photon yield about 3 times higher than that of the original Lipo@IR780/L012 compound at 470 nm. This approach demonstrates how multi-stage amplification strategies can overcome key challenges in organic mechanoluminescence, particularly for biomedical applications requiring both deep penetration and high spatiotemporal control (Fig. 2d).

Researchers have also investigated near-infrared (NIR) imaging of mechanoluminescence. A study by Song *et al.* used PNCL, a NIR chemiluminescent probe, which was designed by combining protoporphyrin IX (PPIX) as a sonosensitizer with an enol-ether precursor of Schaap's dioxetane containing a dicyanomethyl chromone (DCMC) acceptor scaffold (NCL) (Fig. 2f).[57] Their result showed that NIR chemiluminescent molecules hold great potential in organic ML methods, offering deep tissue penetration, high signal-to-background ratios, and non-invasive activation. Ultrasound-induced NIR luminescence provides selective and localized imaging with minimal background noise that reaches depths of up to 20 mm, surpassing visible-light-based techniques. Additionally, NIR mechanoluminescence offers higher sensitivity, reduced phototoxicity, and prolonged signal stability, making it ideal for imaging applications. These molecules are generally biocompatible and, when encapsulated with PEG-based materials, are naturally eliminated over time due to improved solubility and reduced nonspecific tissue interactions. NIR wavelengths were able to achieve deeper penetration, higher signal-to-background ratio, and reduced phototoxic effects, making them a promising direction for further mechanoluminescent applications.[58,59]

Meanwhile, the research group headed by Prof. Tan showed that certain organic nanoparticles, such as TD NPs, can perform the 2-step energy transfer within the same compound.[44] Ultrasonic vibration of TD NPs generate polarization charges through the piezoelectric effect, triggering the production of ROS, which then oxidize TD molecules, forming intermediates such as TD–˙OH and dioxetane compounds. The dioxetane intermediates gradually break down, while TD–˙OH intermediates react with oxygen, causing bond rupture and releasing chemical energy. This energy is transferred to neighboring TD molecules, resulting in luminescence (Fig. 2g). In these methods, the intensity of the resulting light emission is found to be linearly related to the intensity of the ultrasound and ROS generation. Therefore, manipulations to this method have been researched. For instance, including more ROS generating particles and increasing pH, and have shown to achieve stronger luminescent intensity, meanwhile coupling these organic MLNPs with quenchers that absorb luminescence can be used for selective detection.

2.3 Advancement in organic mechanoluminescence

Recent advancements in organic mechanoluminescent nanoparticles have focused on improving brightness and depth through molecular engineering and hybridization strategies. The most promising developmental directions are fine-tuning emission properties through structural modifications for enhanced intensity, extended emission duration, and specificity.[60] Meanwhile, other advances such as ultrasound-activated luminescent probes have enabled highly selective deep-tissue imaging for biomedical applications. Yao *et al.* introduced a dual-locked probe, DPA–H_2S, which utilizes H_2S-activated sonoafterglow luminescence for the precise detection of metformin (MET)-induced liver injury.[61] This probe integrates protoporphyrin IX (PPIX) as the sonosensitizer and a DCMC-based dioxetane precursor, which serves as an afterglow substrate with two activation locks. The first lock, a 2,4-dinitrobenzene group, is selectively cleaved by elevated hepatic H_2S, forming an intermediate (DPA–$^1O_2$), while the second lock, an electron-rich double bond, reacts with ROS to generate an unstable dioxetane, ultimately emitting a NIR afterglow signal ($\sim$710 nm).

Previous probe systems used only one lock and stimuli, which face issues regarding nonspecific activation in complex *in vivo* environments. Meanwhile, this dual-activation strategy ensures that the afterglow is only turned on in the presence of both H_2S and US irradiation, minimizing background noise and enhancing specificity. These findings demonstrate the potential of ultrasound-activated probes for noninvasive, high-resolution imaging and highlight the clinical utility of DPA–H_2S in detecting and monitoring drug-induced liver injury.

3 Organic mechanoluminescent nanoparticles for neuromodulation

Neuromodulation is a technique that alters nerve activity through targeted stimulation using electrical, magnetic, chemical, optogenetic, or ultrasound-based methods. The first practice of neuromodulation was in 1938, when Cerletti *et al.* developed electroconvulsive therapy (ECT) as a treatment for severe psychiatric disorders.[62] Electrical stimulation, such as deep brain stimulation (DBS), spinal cord stimulation (SCS), and vagus nerve stimulation (VNS), delivers controlled impulses to specific neural regions to treat disorders like Parkinson's disease, chronic pain, and epilepsy.[63–65] Magnetic stimulation, including transcranial magnetic stimulation (TMS), non-invasively modulates brain activity and is commonly used for depression and neurorehabilitation.[66] Chemical neuromodulation involves pharmacological agents or direct drug infusion, while optogenetics utilizes light-sensitive proteins to control genetically modified neurons with high precision.[67] Currently, focused ultrasound stimulation (FUS) is the most common way of applying mechanical force as a stimulus for neuromodulation.[68] FUS offers non-invasive ways to influence deep-brain structures with high spatial resolution. Unlike electrical or optogenetic methods, sono-optogenetic methods can penetrate the skull without requiring surgery, making it

a promising, precise, and minimally invasive approach for both therapeutic applications and neuroscience research.

3.1 Sono-optogenetic neuromodulation

Sono-optogenetics is a novel form of neuromodulation inspired by its predecessor, optogenetics. Optogenetics has revolutionized neuroscience by enabling precise control of neuronal activity through genetically encoded light-sensitive ion channels.[69] Most importantly, optogenetics faces tissue penetration challenges due to absorption by naturally occurring endogenous chromophores, such as flavins, hemoglobin, and melanin, as well as light scattering in brain tissue, which limits its applications in deep-brain regions. Many efforts have been made to advance both the targeting strategies and opsins involved in optogenetics. Meanwhile, sonogenetics is another recently developed field that uses FUS to achieve cell-type targeting in genetically modified neurons, which express mechanically sensitive ion channels.[68] Through targeted FUS, sonogenetics can achieve sub-millimeter special resolution and sub-second temporal resolution. However, sonogenetics still faces significant challenges, including off-target effects to the peripheral auditory system, and limited control over inhibition *vs.* excitation.[70,71] Through the combination of ultrasound and optogenetics in sono-optogenetics, researchers aim to achieve a less-invasive and more precise method of neuromodulation.

The mechanism of trap-controlled luminescence is typically seen in inorganic nanoparticles or organic/inorganic hybrids and was first introduced by Xu *et al.* in 1999.[72] Trap-controlled mechanoluminescence occurs through two mechanisms: piezoelectric luminescence and piezo-induced carrier detrapping. In the first, mechanical stress generates a piezoelectric field that directly excites charge carriers, leading to recombination and light emission. In the second, stress modifies the material's energy landscape, releasing previously trapped carriers that then recombine and emit light (Fig. 3a).[53] These mechanisms were capable of intense and reproducible ML, marking its use in sono-optogenetics.

The earliest method of sono-optogenetics leverages trap-controlled mechanoluminescence and ultrasound to activate light-emitting nanoparticles for neural stimulation. Unlike

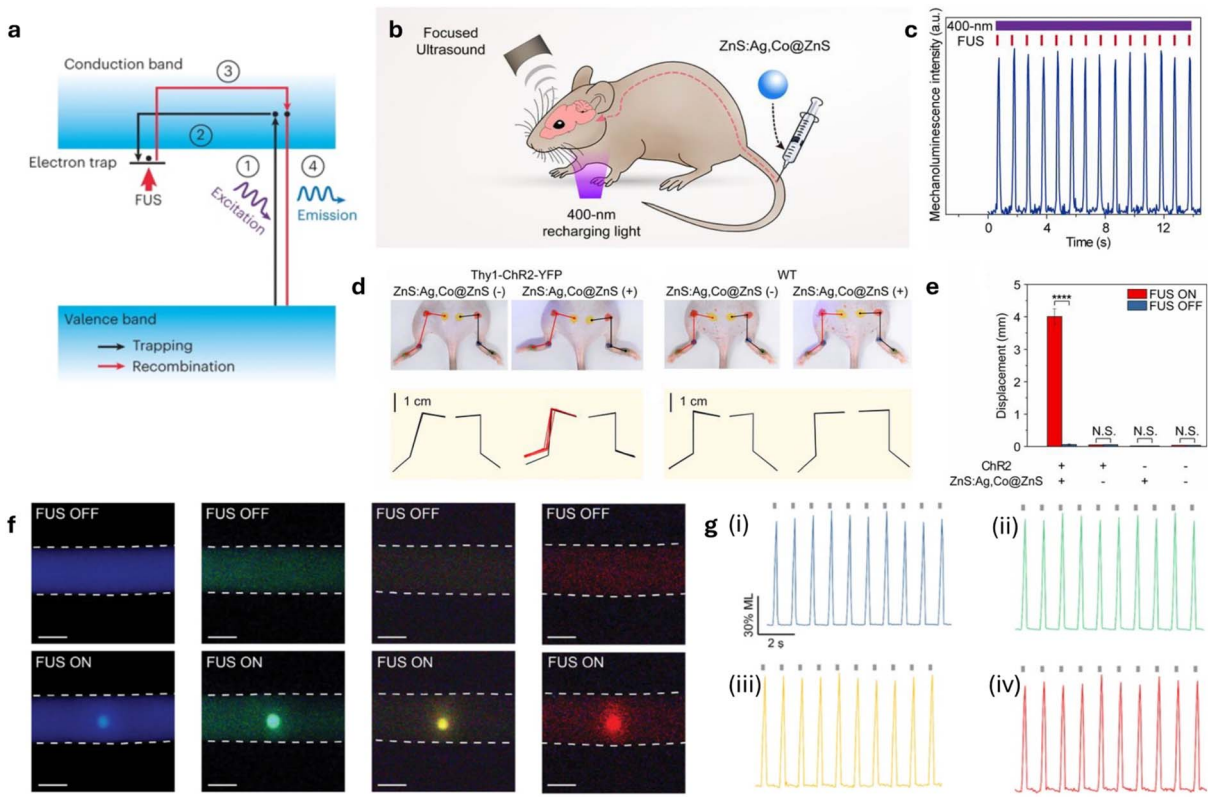

Fig. 3 The development of inorganic mechanoluminescent nanoparticles and their applications in sono-optogenetics. (a) Schematic of trap-controlled mechanoluminescence mechanism. Reproduced with permission from ref. 54. Copyright 2023, Nature Protocols. (b) Schematic illustration of *in vivo* sono-optogenetic stimulation. (c) Intensity of 470 nm emission from ZnS:Ag,Co@ZnS nanoparticles under repeated FUS stimulation (red ticks) and 400 nm recharging light (violet bar) in an artificial circulatory system. (d) Image of Thy1–ChR2–YFP mouse and WT mouse before and after sono-optogenetic stimulation, diagrams showing starting position and maximum range of motion shown for each hindlimb. (e) Statistics of left hindlimb displacement in different groups. Panel (b–e) reproduced with permission from ref. 23. Copyright 2019, National Academy of Sciences, licensed under CC BY 4.0. (f) True color images of tubing containing fluids composed of various ML materials, $Sr_2MgSi_2O_7$:Eu,Dy (blue), ZnS:Cu,Al (green), ZnS:Mn (yellow), and $CaTiO_3$:Pr (red). (g) Representative dynamics of light emission intensity from fluids composed of various ML materials; $Sr_2MgSi_2O_7$:Eu,Dy (i), ZnS:Cu,Al (ii), ZnS:Mn (iii), and $CaTiO_3$:Pr (iv). Panel (f and g) reproduced with permission from ref. 37. Copyright 2022, American Chemical Society.

traditional optogenetics, which faces tissue penetration limitations, mechanoluminescence-based approaches generate light *in situ*, bypassing the need for external fiber optics. Sono-optogenetics methods first introduced by Hong *et al.* uses ZnS:Ag,Co@ZnS nanoparticles as sources for mechanoluminescence, which are injected into the mouse's tail and charged using a 400 nm UV light (Fig. 3b).[23] Upon ultrasound excitation, ZnS:Ag,Co@ZnS produces sufficient to excite ChR2-expressing neurons (Fig. 3c).[28,73] Upon excitation of the ChR2-expressing neurons in motor cortex, hindlimb movement was detected (Fig. 3d). This hindlimb displacement only occurred in the presence of ultrasound, ZnS:Ag,Co@ZnS nanoparticles and ChR2-expressing neurons, showing that displacement was directly motivated by this sono-optogenetic mechanism (Fig. 3e). Furthermore, four stable colloidal solutions were later created containing ML nanocrystals with emissions ranging from 470 nm to 610 nm in response to ultrasound stimulation (Fig. 3f).[32] Multicolored emissions were achieved by selecting specific host materials that exhibit ML properties, such as $Sr_2MgSi_2O_7$:Eu,Dy (blue), ZnS:Cu,Al (green), ZnS:Mn (yellow), and $CaTiO_3$:Pr (red) (Fig. 3g). These materials were synthesized at high temperatures and then processed to form stable, water-soluble nanocrystals while maintaining their ML properties. These ML fluids act as systemically delivered light sources triggered by FUS and can be recharged by photoexcitation.

In sono-optogenetics, nanoparticles remain in circulation and do not need to cross the blood–brain barrier (BBB), as their emitted light can penetrate neural tissue up to 200 μm. The development of sono-optogenetics is a critical technology that has sparked new avenues of research in neuromodulation. This technique would especially benefit from organic mechanoluminescence, as replacing these metal nanoparticles with organic counterparts offers advantages in biocompatibility and biodegradability, addressing concerns about heavy metal accumulation. Organic materials can be chemically tuned to emit light at specific wavelengths, optimizing compatibility with opsins and potentially improving penetration depth for deeper neuromodulation. Additionally, their tunable properties may enhance circulation time and metabolic clearance, reducing long-term retention risks and associated complications.

3.2 Organic mechanoluminescence in neuromodulation

Organic nanoparticles are emerging as versatile tools for neuromodulation, offering tunable physicochemical properties, biocompatibility, and the ability to interface with neural tissues through a range of optical, mechanical, and chemical mechanisms.[29] In 2023, Wang *et al.* developed a biocompatible mechanoluminescence system with enhanced stability, biocompatibility, and systemic circulation for neuromodulation. The system, Lipo@IR780/L012, was fine-tuned to achieve an optimal particle size (~100 nm), promoting prolonged circulation through the bloodstream after intravenous injection. *In vitro* tests revealed that upon ultrasound stimulation, blue mechanoluminescence (~470 nm) activates light-sensitive opsins such as ChR2 and CheRiff. CheRiff channels are activated by 470 nm light emitted from Lipo@IR780/L012 nanoparticles, allowing Ca^{2+} influx into the cells, where it binds to jREGCO1a proteins to amplify the red fluorescence signal of spiking HEK cells.[28] Increased photon density was detected upon FUS irradiation, which spiked the spiking HEK cells. Fluorescence signal recording from CheRiff-expressing spiking HEK cells revealed that reliable signal spikes occurred in the presence of Lipo@IR780/L012 at 100 ms on, 900 ms off FUS pulses. *In vitro* studies showed that the fluorescence signal of spiking HEK cell reliably only spiked in conditions where Lipo@IR780/L012 and FUS were both present (Fig. 4a). *In vivo* studies in Thy1–ChR2–YFP transgenic mice with ChR2 expressing neurons confirmed that motor cortex neurons were temporarily and reversibly activated following intravenous injection and repeated FUS exposure. Excellent biosafety and biocompatibility data make this system a promising approach for minimally invasive, genetically targeted deep brain modulation.

Past the motor cortex, deeper stimulation of the VTA was achieved through a cascade amplification system involving Lipo@IR780/L012/CaO_2.[41] The addition of CaO_2 enabled the production of additional ROS in the form of H_2O_2 and $Ca(OH)_2$, and the increased local concentration of ROS and pH improved the luminescent yield of L012. This model was tested *in vivo*, where head-fixed mice received an intracranial injection of the Lipo@IR780/L012/CaO_2 and were placed into the lever-pressing paradigm 24 hours later. When the mice pressed the ultrasound trigger, the FUS transducer generated a single ultrasound pulse that stimulates the reward-seeking behavior of the mouse brain. It was found that Thy1–ChR2–YFP transgenic mice, when injected with Lipo@IR780/L012/CaO_2 and received FUS stimulation upon pressing the lever, increased lever pressing rates throughout the trial (Fig. 4b).

In 2025, Wang *et al.* reported a new approach that can treat Parkinson's disease in a rat model. A hemiparkinsonian model of the rat was created through treatment from stereotaxic injection of 6-hydroxydopamine (6-OHDA) into the medial forebrain bundle (MFB) region and confirmed through the cylinder test. The approach used hydrogen-bonded organic frameworks (HOF), where ultrasound activation of PV-GPe neurons led to significant motor symptom alleviation comparable to conventional optogenetics, as validated by an apomorphine-induced rotation test and the time-resolved rat rotation angular displacement.[42] The results achieved through sono-optogenetics were comparable to that of optogenetics (Fig. 4c), highlighting the broader applicability of mechanoluminescence in non-invasive photon delivery systems for optogenetics, gene regulation, immunotherapy, and bioimaging. Further improvements in FUS spatial resolution will be critical for achieving submillimeter precision in neuromodulation. Additionally, the refinement of organic sonosensitizers and chemiluminescent substrates could improve mechanoluminescence efficiency and spectral tuning, broadening the potential for precise and noninvasive neural circuit modulation.

Organic MLNPs offer significant advantages for neuromodulation, particularly due to their excellent biocompatibility, flexibility, and seamless integration with biological tissues.

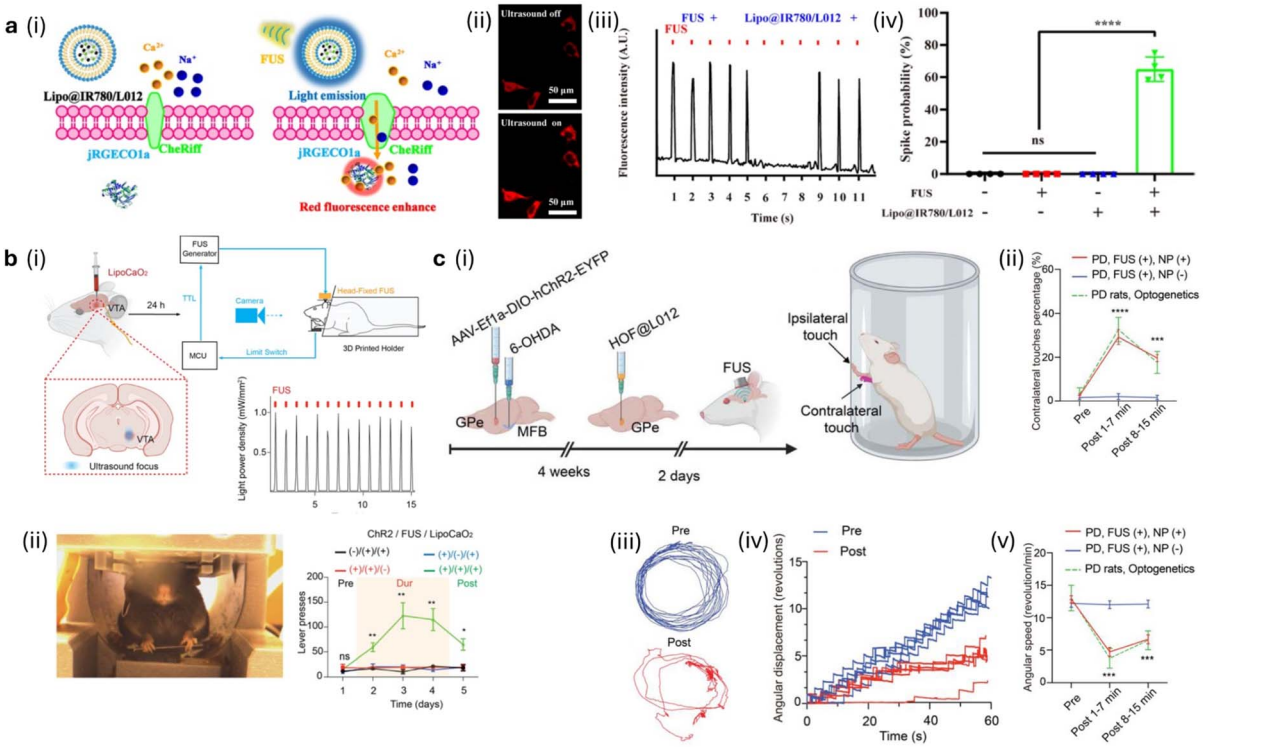

Fig. 4 Ultrasound-triggered mechanoluminescence for noninvasive sono-optogenetics in spiking HEK cells, activation of VTA region of a mouse and the following lever press test and the rat's Parkinson model. (a) Scheme of FUS-triggered CheRiff channels upon 470 nm blue light exposure from Lipo@IR780/L012 nanoparticles. Ca^{2+} enters the cell through CheRiff channels and enhances red fluorescence signal upon binding with jREGCO1a proteins (i). Fluorescence images of CheRiff-expressing spiking HEK cells with and without ultrasound stimulation (ii). Fluorescent intensity with FUS and Lipo@IR780/L012 nanoparticles (iii). Spike probability of spiking HEK cells under the different conditions of FUS and Lipo@IR780/L012 (iv). Reproduced with permission from ref. 41. Copyright 2023, American Chemical Society. (b) Schematic (i) of lever press mechanism for sono-optogenetic testing. A FUS pulse is initiated when the mouse pulls the lever (i). Total lever presses for different mouse conditions over time (ii). Reproduced with permission from ref. 31. Copyright 2023, American Chemical Society. (c) Scheme of hemi-parkinsonian model rat for PV-GPe sono-optogenetics (i) and assessment using cylinder test (ii). Apomorphine-induced rotation tests before and after FUS stimulation (iii). Rat rotation angular displacement during the rotation test before and after stimulation over time (iv) and comparison of angular speed results from sono-optogenetics methods and optogenetics (v). Reproduced with permission from our previous work ref. 42. Copyright 2025.

These materials enable minimally invasive or non-invasive neuromodulation, as they can be delivered through the bloodstream and remotely activated by external stimuli such as ultrasound. Compared to conventional optogenetics, which often requires surgically implanted optical fibers that lead to tissue damage and gliosis, sono-optogenetics can serve as internal light sources activated by mechanoluminescence, reducing the need for invasive procedures.[23,74] Meanwhile, integration of artificial intelligence and closed-loop control systems, as proposed by Yang *et al.*, provide real-time adaptive feedback to lower energy consumption and increase efficacy.[75] Beyond the brain, this technology could be applied to neuromodulation in harder-to-access organs such as the heart and lungs. Ongoing research aims to increase the emission intensity and efficiency of organic mechanoluminescent materials, optimizing molecular design to increase rigidity and electron delocalization while decreasing decay and quenching. In addition, future systems could incorporate multimodal capabilities, combining neuromodulation with other biomedical functions such as real-time imaging or drug delivery. As research in organic mechanoluminescence and neuromodulation progresses, these materials hold promise for transforming both research and clinical neuromodulation, offering more precise, customizable, and patient-friendly therapeutic options.

4 Organic mechanoluminescence in bioimaging

Bioimaging techniques are essential for visualizing biological processes, diagnosing diseases, and advancing medical research. Traditional bioimaging modalities, such as magnetic resonance imaging (MRI), computed tomography (CT), and positron emission tomography (PET) have played a critical role in clinical and research applications. However, PET scans are generally poor at imaging anatomic detail and results in bad localization of lesions. CT scans have high energy requirements and costs as well as risk to tissue due to radiation.[76,77] On the other hand, MRI faces challenges such as difficult setup, high costs, long imaging time.[78,79] Meanwhile, alternatives such as bioluminescence and chemiluminescence face significant

limitations, including restricted imaging depth, light scattering, photobleaching, and spatial resolution constraints.[80,81] These limitations hinder the development of non-invasive, high-resolution imaging systems capable of real-time, deep-tissue molecular imaging. To overcome these challenges, ultrasound-enhanced bioimaging has emerged as a promising alternative for enhanced precision, higher spatiotemporal resolution, and increased depth. Recent advancements in organic ML materials have further expanded the potential of ultrasound-enhanced bioimaging, enabling high-sensitivity molecular imaging and deep-tissue visualization. This section explores the development and application of organic MLNPs in bioimaging, emphasizing its advantages in molecular imaging and tissue imaging.

4.1 Organic mechanoluminescence for molecular imaging and disease diagnosis

Ultrasound-enhanced bioimaging has emerged as a promising technique for improving spatial resolution, sensitivity, and deep tissue penetration in medical imaging. The integration of ultrasound with chemiluminescence has been validated through theoretical models, tissue mimics, and *in vivo* studies, demonstrating significant improvements in spatial information and reduced light scattering. Earlier studies have found that ultrasound at frequencies of 3 MHz or intensities above 5 W cm^{-2} significantly enhances chemiluminescence signals, enabling tissue imaging at depths of up to 30 mm with a resolution of 2 mm.[81]

In 2022, Prof. Pu *et al.* designed sonoafterglow nanoparticles (SNAPs), as a cutting-edge technique that enhances deep-tissue optical imaging by significantly reducing background noise and increasing signal-to-noise ratio.[40] The imaging process begins with the systemic administration of SNAPs, which passively accumulate in target tissues due to the enhanced permeability and retention (EPR) effect. Once localized, the sonoafterglow signal is activated by ultrasound that initiates a molecular cascade that enables long-lasting luminescence independent of continuous external irradiation. The depth-resolved imaging capability of SNAPs is a major advancement over traditional optical imaging modalities. Unlike fluorescence or photo-afterglow imaging, which were limited to depths of 1–2 cm, sonoafterglow signals can be detected at depths of up to 4 cm due to the deep tissue penetration properties of ultrasound. Additionally, this method is superior to fluorescence imaging, which suffers from autofluorescence and rapid signal decay. Imaging is typically performed using an *in vivo* imaging system (IVIS) with bioluminescence detection settings, ensuring high sensitivity and minimal interference from surrounding tissues. The emitted afterglow, primarily in the NIR spectrum (around 780 nm), ensures optimal tissue penetration while minimizing scattering and absorption. The use of organic MLNPs benefits from renewable and repeatable luminescence, enabling real-time tracking of dynamic biological processes such as immune response activation and tumor progression. The combination of high specificity, deep tissue penetration, and sustained signal duration makes SNAPs a powerful tool for *in vivo* molecular imaging, particularly in applications such as tumor detection, drug activation monitoring, and real-time assessment of therapeutic responses. A key advantage of SNAPs in bioimaging is their ability to be molecularly engineered to respond selectively to specific biomarkers. SNAP-M is a sonoafterglow probe that incorporates substrates such as peroxynitrite ($ONOO^-$)-responsive dioxetanes to SNAP, allowing imaging to correlate directly the biomarker $ONOO^-$, which indicates a pro-inflammatory tumor microenvironment.[40] SNAP-M was validated for the deep-tissue (>2 cm) evaluation of M1 macrophages during immunotherapy.

Furthermore, ultrasound-triggered persistent luminescence for enzyme probing is another emerging possibility. The Pu group used the sonosensitizer NCBS and substrate DPA to develop a quencher mechanic sonoafterglow nanoprobe (Q-SNAP), to detect the presence of specific enzymes (Fig. 5a).[82] Luminescence quenchers are connected to the SNAP compound through a granzyme B (GZMB) cleavable peptide. Only in the presence of GZMB are quenchers liberated from Q-SNAP, allowing emission of luminescence in the presence of T cells. This model was tested *in vivo* through in murine concanavalin (ConA)-induced hepatitis, to mimic human autoimmune hepatitis (Fig. 5b). Upon intravenous injection of Q-SNAP, *in vivo* fluorescence and sonoafterglow imaging demonstrated that luminescence in the liver region of ConA-treated mice was significantly higher in intensity than that of the control phosphate-based saline (PBS) and that of CysA–ConA treatments (Fig. 5c and e). Additionally, sonoafterglow for the ConA treatment exhibited the highest signal-to-background ratio, as well as the highest fluorescent and sonoafterglow intensity (Fig. 5d, f and g). These results show that quencher-mechanism MLNPs are valuable for detecting enzyme activity *in vivo* with high sensitivity and specificity. Their ability to provide ultrasound-triggered persistent luminescence offers a promising avenue for molecular imaging applications, particularly in monitoring immune responses, tracking disease progression, and assessing therapeutic efficacy in real time.

Similarly, in 2024, the Tan group's trianthracene derivative-based nanoparticles (TD NPs) also achieved similar bioimaging uses.[44] The light produced as a result was found to penetrate at least 2.2 cm deeper than that of fluorescent imaging, a spatial resolution of 1.46 mm with 0 mm of tissue, as well as a signal-to-noise ratio of 206, far surpassing that of fluorescence by 11.7 times. Meanwhile, PFODBT doping with HBA–COOH was also found to enhance luminescence intensity. Tan then developed and utilized enzyme-cleavable peptide sequences as molecular switches to control luminescence output. By linking a luminescent donor nanoparticle (TD NPs) to a quencher (BHQ-3) *via* an enzyme-cleavable peptide, the system remains in a quenched, non-luminescent state until the target enzyme cleaves the peptide (Fig. 5h). This cleavage physically separates the donor and quencher, restoring luminescence and providing a direct optical readout of enzymatic activity. For example, a granzyme B-specific probe TD–Grz–BHQ uses the peptide sequence IEFD, which is selectively cleaved by granzyme B, releasing the quencher and triggering detectable luminescence. TD–Grz–BHQ was tested for distinguishing the immune response after

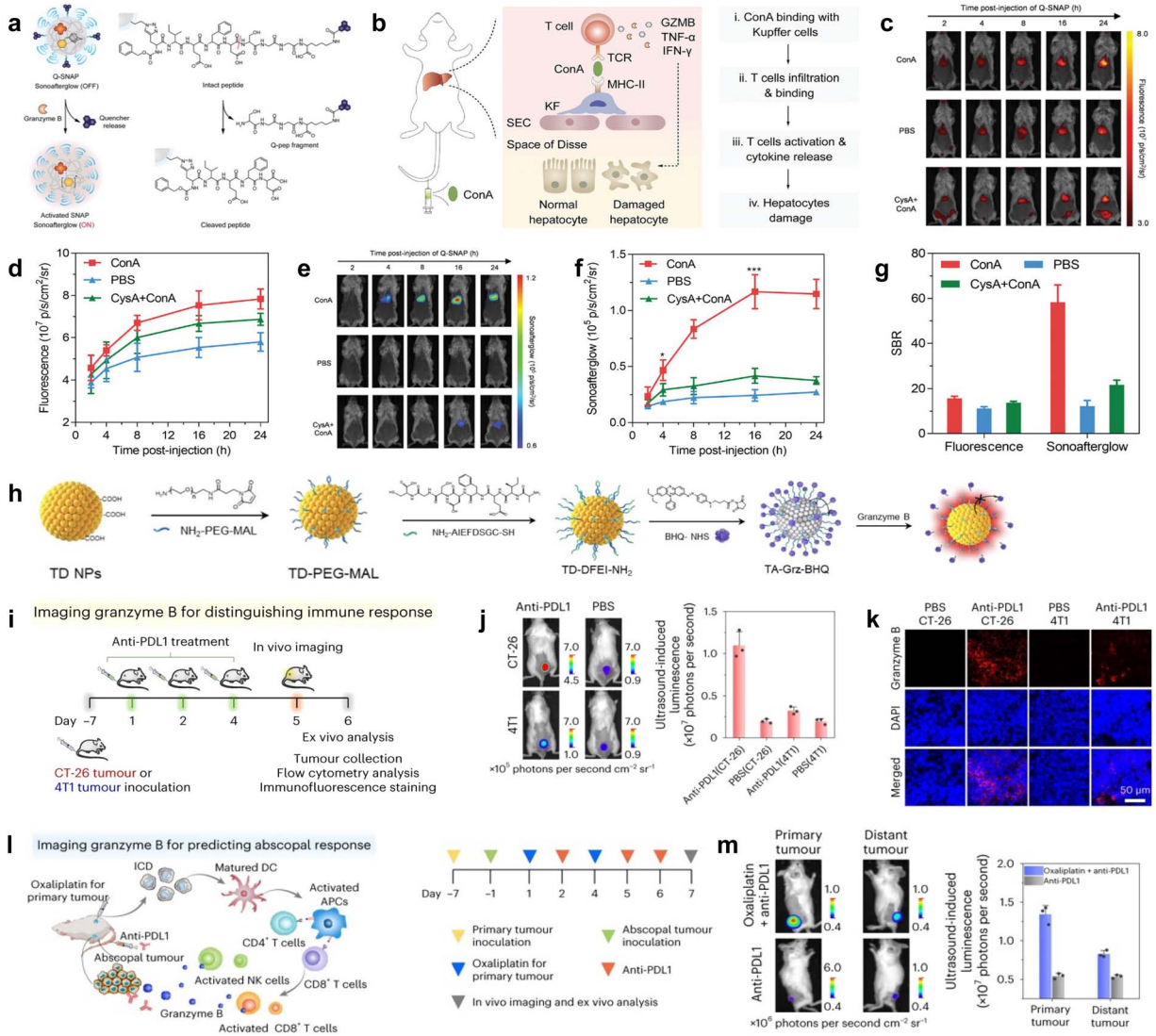

Fig. 5 Mechanoluminescence-induced imaging for molecular and diagnostic applications. (a) Schematic of Q-SNAP sonoafterglow as activated by GZMB. (b) Schematic of ConA-induced hepatitis model in mouse. (c) *In vivo* fluorescence of mice at time points after Q-SNAP injection. (d) Fluorescent intensities of liver region panels. (e) Sonoafterglow images of mice at time points after Q-SNAP injection. (f) Sonoafterglow intensities of liver region panels. (g) Signal-to-background ratio (SBR) at maximum intensities of fluorescence and sonoafterglow. Panel (a–g) reproduced with permission from ref. 82. Copyright 2023, Wiley-VCH. (h) Schematic of activatable ultrasound-induced luminescence probes imaging enzyme. (i) Schematic of TD–Grz–BHQ imaging distinguishing immune response of different tumor types. (j) Images and intensities of luminescence after injection with TD–Grz–BHQ. (k) Fluorescence images of tumor slices stained with granzyme B antibody and DAPI. (l) Schematic diagram of abscopal effect induced by oxaliplatin and anti-PDL1 and administration procedure for granzyme-B imaging. (m) Delayed ultrasound-induced luminescence images and intensities of primary and metastatic tumors. Panel (h–m) reproduced with permission from ref. 44. Copyright 2024, Springer Nature.

anti-programmed cell death ligand 1 (anti-PDL1) treatment in two tumor models, CT-26 and 4T1, 5 days after the first anti-PDL1 treatment (Fig. 5i). When the TDNPs-injected tumors were excited with ultrasound, they exhibited strong luminescence, while almost no background signal was detected with a ~206 signal-to-noise ratio, 11.7-fold higher than that of fluorescence (Fig. 5j and k). The particles also determined abscopal response in mice receiving oxaliplatin combined with anti-PDL1 treatment (Fig. 5l), and identified metastatic tumors (Fig. 5m). This design has enormous potential for biomedical applications, including monitoring tumor immune responses, assessing drug-induced hepatotoxicity by detecting liver enzyme activation, and enhancing tumor and lymph node detection. The combination of enzyme specificity with the spatial and temporal precision of ultrasound-induced luminescence imaging makes these probes especially attractive for noninvasive diagnostics and precision medicine approaches.

Despite its advantages, ultrasound-enhanced bioimaging faces challenges. Specifically, the heat generated by focused ultrasound scales with ultrasound intensity, which can pose risks of tissue damage if temperatures exceed the threshold of 42 °C for just a minute of exposure.[83] To mitigate these risks,

research has focused on optimizing exposure duration, with short bursts of high-intensity focused ultrasound (HIFU) proving effective in limiting temperature increases. In the future, the integration of drug-loaded microbubbles with nanoparticle probes may enable theranostics applications, where ultrasound stimulation facilitates both imaging and targeted therapeutic delivery.[84] As research continues, its translational potential for physiological imaging, cancer diagnostics, and molecular imaging is expected to grow, paving the way for more accurate and minimally invasive diagnostic tools.

4.2 Organic mechanoluminescence for therapeutic applications

An example of the use of organic MLNPs in cancer interventions include sonoafterglow cancer nanoimmunotheranostics (SCAN), which was developed by Pu's group by incorporating a silenced immune prodrug (Pro-R837) into SNAP.[40] SCAN were developed with a dual-locked activation mechanism, incorporating Pro-MB, a silenced sonoafterglow initiator activated by $ONOO^-$, and Pro-R837, an M1-polarizing prodrug cleaved by $^1O_2$ (Fig. 6a and b). Upon ultrasound application, $ONOO^-$-activated SCAN generated $^1O_2$, leading to sonoafterglow emission and immune activation. *In vitro* testing demonstrated that without $ONOO^-$, SCAN had no therapeutic effect, but once activated, it induced 78.1% cancer cell death under ultrasound stimulation (Fig. 6c). Further analysis showed that activated SCAN significantly repolarized M2 macrophages into M1 macrophages, eliciting a 4.4-fold higher M1 population compared to PBS treatment and a 3.1-fold increase compared to non-activated SCAN (Fig. 6d). Moving to *in vivo* experiments, systemic SCAN administration in a 4T1 tumor-bearing mouse model allowed for tumor imaging *via* sonoafterglow, followed by ultrasound-triggered immune activation (Fig. 6e and f). Multiple doses of SCAN progressively enhanced the pro-inflammatory tumor microenvironment, as indicated by increasing sonoafterglow intensity, with a 4.82-fold increase after the second dose (Fig. 6g) and an additional 1.74-fold increase after the third dose (Fig. 6h). Ultimately, ultrasound-mediated SCAN therapy successfully inhibited tumor growth, leading to tumor eradication and prolonged survival in treated mice. This dual-lock mechanism requires both ultrasound and peroxynitrite ($ONOO^-$), ensuring precise, localized activation while avoiding off-target effects common in conventional nanoimmunotheranostic agents. Additionally, this strategy significantly reduces the required drug dosage compared to traditional toll-like receptor agonist-loaded nanoparticles.[85] The

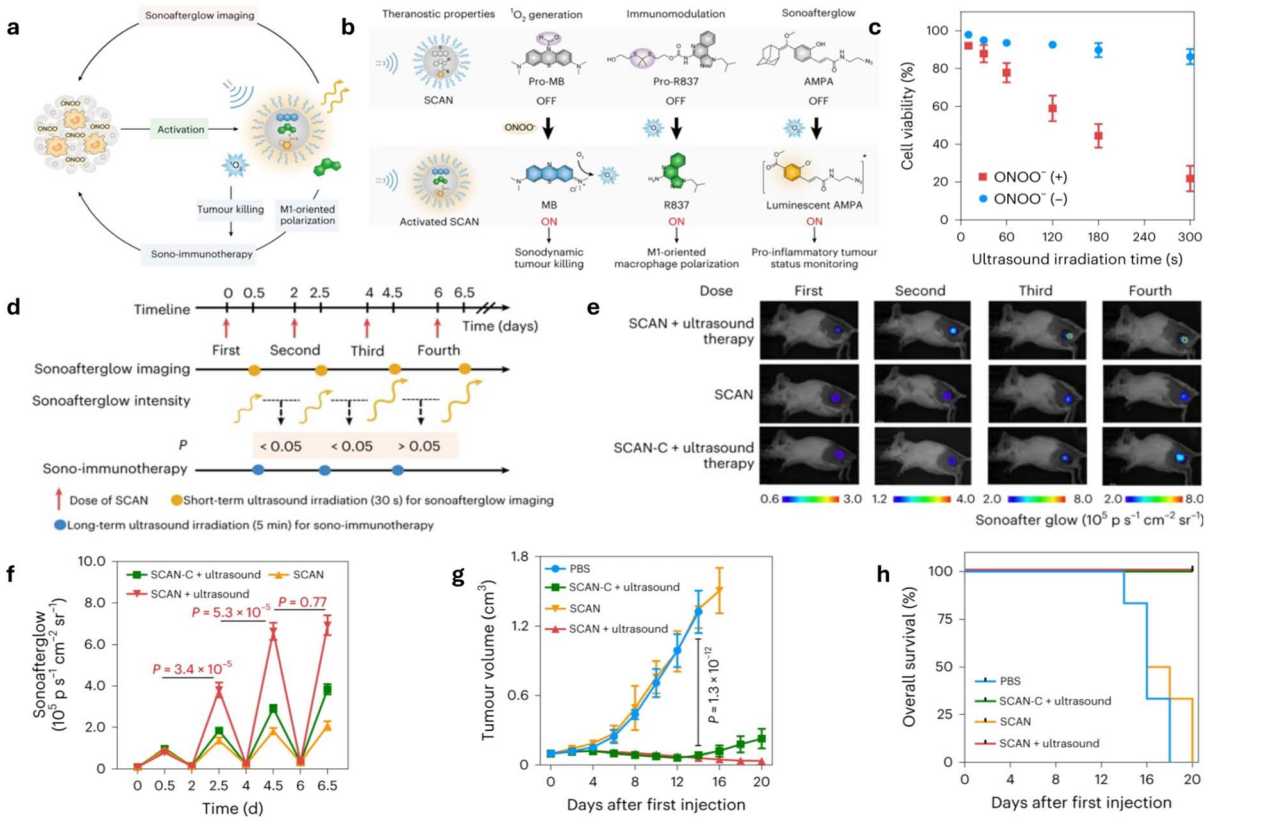

Fig. 6 Organic mechanoluminescent-induced cancer therapeutics. (a) Scheme of SCAN for sonoafterglow-guided cancer immunotherapy. (b) Scheme of SCAN molecular mechanism for sonoafterglow cancer immunotheranostics. (c) Viability of 4T1 cancer cells and $ONOO^-$ treated and untreated SCAN upon ultrasound stimulation. (d) Timetable of sonoafterglow immunotherapy on 4T1 tumor-bearing mice. (e) Images of sonoafterglow on tumors at 0 and 0.5 h after SCAN-C and SCAN therapy. (f) Intensity of sonoafterglow on tumors at 0 and 0.5 h after SCAN-C and SCAN therapy. (g) Tumor growth curves and (h) mice survival curves after indicated treatments. All panels reproduced with permission from ref. 3. Copyright 2023, Springer Nature.

success of SCAN highlights the broader potential of sonosensitizers and organic mechanoluminescent materials in theranostics, demonstrating their ability to achieve non-invasive, deeply penetrative, and precisely controlled therapeutic interventions.

Furthermore, organic MLNPs can be used for therapeutics that require light emission. For instance, photodynamic therapy (PDT) is a minimally invasive treatment modality that uses photosensitizers activated by specific wavelengths of light to generate ROS inducing localized cytotoxicity and cell death.[86] Recent advancements in photodynamic therapy (PDT) have focused on overcoming two major limitations: the dependence on oxygen and the need for high-intensity light to activate photosensitizers. A study by Tang *et al.* in 2024 introduced an oxygen-independent organic photosensitizer capable of generating superoxide and hydroxyl radicals even in hypoxic tumor environments, significantly boosting ROS production.[87] While this work utilizes a photosensitizer, the underlying design principles of enhancing molecular interactions and optimizing ROS generation efficiency inform future development of sonosensitizers and organic MLNPs, which could enable mechanically triggered PDT without external light sources. Such approaches hold promise for minimally invasive, site-specific cancer therapies, particularly for deep-seated or hypoxic tumors.

One of the key advantages of ML over other luminescence-based techniques, such as fluorescence or bioluminescence, is its ability to activate luminescent contrast agents on demand with precise spatial and temporal control to overcome issues like signal diffusion and background noise. Furthermore, organic ML bioimaging enables deeper tissue imaging while also avoiding tissue autofluorescence compared to traditional optical methods. Current research explores the use of organic ML probes for cancer imaging, tissue assessment, and targeted drug localization with promising data showing enhanced imaging resolution and signal persistence. Preclinical models have demonstrated the potential to visualize tumor microenvironments, detect molecular markers of disease, and monitor treatment responses dynamically, paving the way for improved diagnostic and therapeutic strategies.

Despite the significant progress made in the development and application of organic ML for biomedical imaging and therapeutic monitoring, several key challenges must be addressed before these technologies achieve widespread clinical adoption. Fundamental mechanisms underlying persistent luminescence activation, particularly in ultrasound-triggered systems, remain poorly understood, limiting rational design of next-generation particles with optimized performance. Furthermore, ultrasound excitation also presents challenges related to tissue heating and inconsistent activation efficiency. Future research in organic MLNPs will prioritize their design with enhanced biocompatibility, minimized toxicity, and improved activation sensitivity under clinically safe conditions. With continued interdisciplinary innovation, organic ML hold the potential to revolutionize bioimaging.

5 Prospective applications and future outlook

5.1 Organic mechanoluminescence for optophysiology

Optophysiology is the study and manipulation of cellular physiology using optogenetic tools, typically light-activated molecular switches that allow for the precise control of biological processes with high spatial and temporal resolution. This rapidly growing field has revolutionized how researchers investigate cellular behavior by offering noninvasive, reversible, and highly targeted control over ion channels, signaling pathways, gene expression, cytoskeletal dynamics, and even organelle functions.[88] By leveraging optogenetic systems, scientists can dissect the inner workings of cells in real-time, studying processes such as autophagy, cell cycle progression, transcriptional regulation, and protein degradation with unprecedented precision. The significance of optophysiology lies in its ability to bridge the gap between molecular-scale biochemistry and whole-cell or tissue-level physiology, making it a powerful tool for both basic biological research and translational medicine.

The upcoming advances in brain research and cell function manipulation using optophysiology will be propelled by progress in deep-tissue sono-optogenetics and the development of wireless light delivery systems, enabling minimally invasive optical control in living organisms while bypassing some of the limitations associated with external illumination. Organic MLNPs have shown promise by embedding these materials into biocompatible nanoparticles, researchers could illuminate target cells simply by applying external pressure, opening new avenues for remote, noninvasive control of cellular physiology.

5.2 Organic mechanoluminescence integrating traditional theranostics

Essentially, organic ML is extremely flexible and can be implemented into any biomedical applications involving the delivery of light into tissue. For instance, organic ML offers a unique opportunity to enhance prodrug systems by providing a built-in activation trigger that responds to light stimuli. Organic ML materials could serve both as mechanical sensors and energy donors, where the mechanically induced luminescence provides localized light energy to trigger photochemical prodrug activation or excite luminescent components that initiate downstream chemical reactions. This dual functionality could enable site-specific, non-invasive drug activation, particularly in deep tissues where traditional light sources struggle to penetrate. A recent study by An *et al.* demonstrated this potential by developing a platinum(IV) prodrug system (Pt(IV)–Lu) that takes advantage of endogenous luminescence generated within the tumor microenvironment.[89] The system relies on luminol (Lu), which becomes oxidized in the tumor's ROS rich environment, emitting blue luminescence. This luminescence directly triggers the reduction of Pt(IV) into its active Pt(II) form, which is responsible for the drug's anticancer effects. The study showed that Pt(IV)–Lu remained stable and inactive in normal tissues, but became highly effective in tumor environments, exhibiting strong antitumor efficacy in both *in vitro* and *in vivo* models.

Another emerging area is combining fluorescence with enzyme-mimetic catalytic activity through the development of aggregation-induced emission nanozymes.[90] Organic ML luminophores could be incorporated into similar nanozyme systems, where mechanical stimuli, such as ultrasound, can dynamically activate both luminescence and catalytic activity. These force-responsive nanozymes could function as theranostic tools, capable of both sensing mechanical abnormalities and initiating catalytic therapeutic responses directly at the affected site.

Simultaneously, there have been advancements in the development of biohybrid mechanoluminescent applications. Yang *et al.* introduced a sonosynthesis-based therapeutic platform that integrates ultrasound (US)-activated cyanobacterial photosynthesis with sonodynamic therapy (SDT) using sonoafterglow nanoparticles (NPs-Ce6).[91] These nanoparticles generate ROS and red light upon ultrasound stimulation, activating cyanobacteria to produce oxygen and overcome the tissue penetration limitations of external light. This concept demonstrates how mechanoluminescence can be extended to other biomedical applications using the power of cellular mechanisms. By leveraging mechanical stimuli to generate localized luminescence, this approach offers new possibilities for mechanoluminescent materials in precision medicine and regenerative therapies.

5.3 Current limitations of organic mechanoluminescence

While organic MLNPs show promise for biomedical applications, several challenges must be addressed before clinical translation. In bioimaging, their luminescence intensity is often weaker than inorganic alternatives, potentially limiting detection sensitivity in deep tissues. Although organic nanoparticles generally exhibit better biocompatibility and biodegradability than metal-based systems, their long-term biodistribution, biodegradation pathways, and potential inflammatory responses remain insufficiently studied. While short-term studies in rodents show minimal toxicity after neuromodulation, extended evaluation periods and larger animal models are needed to evaluate effects on the other anatomic systems.[92] In cancer therapeutics, ML nanoparticles may face hurdles in achieving sufficient tumor-specific accumulation while minimizing off-target effects. Their responsiveness to mechanical stimuli offers precise activation, but inconsistent mechanical properties in heterogeneous tumors may lead to uneven therapeutic delivery.[93] Furthermore, the metabolic byproducts of organic ML materials, though less toxic than heavy metals, require detailed long-term testing and toxicity profiling to rule out unwanted side effects and damages.

6 Conclusion

In conclusion, organic mechanoluminescent nanoparticles (MLNPs) have emerged as a groundbreaking class of materials with transformative potential in biomedical applications. Their unique ability to convert mechanical energy into light emission, combined with their biocompatibility, chemical tunability, and compatibility with remote stimuli such as ultrasound, makes them ideal candidates for next-generation diagnostic and therapeutic platforms. Recent advancements have significantly expanded the understanding of organic ML, enabling the rational design of organic MLNPs with tailored emission wavelengths, prolonged afterglow, and enhanced intensity, offering a new level of control over luminescent behavior under mechanical stress.

The development of hybrid organic–inorganic ML systems, isostructural doping strategies, and cascade amplification mechanisms has further broadened the applicability of organic MLNPs by enhancing emission brightness, expanding spectral coverage into the NIR region, and enabling multistage signal amplification. These advances are particularly significant for deep tissue bioimaging, noninvasive neuromodulation, and theranostics applications, where precise spatiotemporal control over light emission is crucial. At the same time, the integration of organic ML with ultrasound technology has revolutionized remote luminescence activation, allowing for non-contact, deep-tissue light generation with exceptional spatial resolution. This progress highlights the versatility of organic MLNPs, ranging from stress sensors and optoelectronic displays to sophisticated biomedical tools capable of imaging, sensing, and therapeutic delivery.

Several challenges remain before the full clinical and technological potential of organic ML can be realized. Issues such as limited long-term photostability, susceptibility to environmental quenching, and the need for highly reproducible material synthesis must be addressed. Additionally, further work is needed to optimize the molecular design of organic ML materials for specific biomedical applications, for instance, balancing emission intensity, wavelength, biocompatibility, and degradability. Therefore, there is still much research needed before moving toward the commercialization and use of these technologies. As research continues to evolve, the convergence of advanced material design, mechanistic insight, and innovative biomedical engineering is expected to establish organic ML as a cornerstone technology for future noninvasive diagnostics, precision neuromodulation, and multimodal imaging systems, ushering in a new era of smart luminescent materials tailored for real-world challenges.

Data availability

No primary research results, software or code have been included, and no new data were generated or analyzed as part of this review. Data available on request from the authors.

Author contributions

C. Gu, X. Liu and H. Wang designed the structure of the review and collected the papers and figures for this review. C. Gu and S. Brian wrote the original draft. X. Liu, W. Wang, W. He and H. Wang supervised the review and revised the manuscript. Finally, the manuscript was revised by all authors.

Conflicts of interest

The authors declare no conflict of interest.

Acknowledgements

This study is supported by the National Science Foundation (NSF) CAREER award (2340964), NIH Maximizing Investigators' Research Award (National Institute of General Medical Sciences 1R35GM147408), Robert A. Welch Foundation Grant, UT Austin Portugal Exploratory Research Projects Grant, Alpha-1 Foundation Pilot and Feasibility Grant, and Craig H. Neilsen Foundation Pilot Research Grant.

References

1 D. R. Vij, *Luminescence of Solids*, Springer Nature, New York, NY, 2012.
2 G. E. Hardy, J. C. Baldwin, J. I. Zink, W. C. Kaska, P.-H. Liu and L. Dubois, *J. Am. Chem. Soc.*, 1977, **99**, 3552–3558.
3 J.-C. Zhang, X. Wang, G. Marriott and C.-N. Xu, *Prog. Mater. Sci.*, 2019, **103**, 678–742.
4 B.-H. Di and Y.-L. Chen, *Chin. Chem. Lett.*, 2018, **29**, 245–251.
5 B. P. Chandra, C. N. Xu, H. Yamada and X. G. Zheng, *J. Lumin.*, 2010, **130**, 442–450.
6 N. Bieniek, S. Inacker and N. Hampp, *Phys. Chem. Chem. Phys.*, 2021, **23**, 17703–17712.
7 G. Blasse, G. J. Dirksen and L. H. Brixner, *Mater. Chem. Phys.*, 1986, **14**, 485–494.
8 L. Li and Y. Zhang, *Nano Res.*, 2017, **10**, 2527–2534.
9 Y. Wen, S. Xiao, H. Liu, X. Tian, J. De, T. Lu, Z. Yang, D. Zou, Y. Lv, S.-T. Zhang, Q. Su and B. Yang, *J. Mater. Chem. C*, 2021, **9**, 17511–17517.
10 L. M. Shaker, A. Al-Amiery and W. N. R. W. Isahak, *Green Technol. Sustainability*, 2024, **2**, 100111.
11 Y. Zhuang and R.-J. Xie, *Adv. Mater.*, 2021, **33**, e2005925.
12 C. Li, Q. He, Y. Wang, Z. Wang, Z. Wang, R. Annapooranan, M. I. Latz and S. Cai, *Nat. Commun.*, 2022, **13**, 3914.
13 C. N. Xu, T. Watanabe, M. Akiyama and X. G. Zheng, *Appl. Phys. Lett.*, 1999, **74**, 1236–1238.
14 H. Zheng, L. Niu, W. Qiu, D. Liang, X. Long, G. Li, Z. Liu and L. Meng, *Research*, 2023, **6**, 0200.
15 Y. Petrov, I. Y. Petrov, R. O. Esenaliev, M. Kinsky and D. S. Prough, in *Photons Plus Ultrasound: Imaging and Sensing 2011*, ed. A. A. Oraevsky and L. V. Wang, SPIE, 2011, p. 78990C.
16 V. J. Robertson and K. G. Baker, *Phys. Ther.*, 2001, **81**, 1339–1350.
17 D. P. Darrow, *Neurotherapeutics*, 2019, **16**, 88–99.
18 M. R. Bailey, V. A. Khokhlova, O. A. Sapozhnikov, S. G. Kargl and L. A. Crum, *Acoust. Phys.*, 2003, **49**, 369–388.
19 J. Ouyang, Z. Tang, N. Farokhzad, N. Kong, N. Y. Kim, C. Feng, S. Blake, Y. Xiao, C. Liu, T. Xie and W. Tao, *Nano Today*, 2020, **35**, 100949.
20 W. Akhtar, M. A. Arain, A. Ali, N. Manzar, Z. Sajjad, M. Memon, W. Memon and N. Ahmad, *J. Ultrasound Med.*, 2011, **30**, 981–985.
21 T. R. Nelson, J. B. Fowlkes, J. S. Abramowicz and C. C. Church, *J. Ultrasound Med.*, 2009, **28**, 139–150.
22 L. Jiang, Y. Yang, Y. Chen and Q. Zhou, *Nano Energy*, 2020, **77**, 105131.
23 X. Wu, X. Zhu, P. Chong, J. Liu, L. N. Andre, K. S. Ong, K. Brinson Jr, A. I. Mahdi, J. Li, L. E. Fenno, H. Wang and G. Hong, *Proc. Natl. Acad. Sci. U. S. A.*, 2019, **116**, 26332–26342.
24 F. Giuntini, F. Foglietta, A. M. Marucco, A. Troia, N. V. Dezhkunov, A. Pozzoli, G. Durando, I. Fenoglio, L. Serpe and R. Canaparo, *Free Radical Biol. Med.*, 2018, **121**, 190–201.
25 R. F. Martínez, G. Cravotto and P. Cintas, *J. Org. Chem.*, 2021, **86**, 13833–13856.
26 A. Marin, M. Muniruzzaman and N. Rapoport, *J. Controlled Release*, 2001, **71**, 239–249.
27 W. Wang, A. Tasset, I. Pyatnitskiy, H. G. Mohamed, R. Taniguchi, R. Zhou, M. Rana, P. Lin, S. L. C. Capocyan, A. Bellamkonda, W. Chase Sanders and H. Wang, *Adv. Drug Delivery Rev.*, 2022, **186**, 114343.
28 W. Wang, X. Wu, K. W. Kevin Tang, I. Pyatnitskiy, R. Taniguchi, P. Lin, R. Zhou, S. L. C. Capocyan, G. Hong and H. Wang, *J. Am. Chem. Soc.*, 2023, **145**, 1097–1107.
29 X. Wu, F. Yang, S. Cai, K. Pu and G. Hong, *ACS Nano*, 2023, **17**, 7941–7952.
30 K. Chang, J. Gu, L. Yuan, J. Guo, X. Wu, Y. Fan, Q. Liao, G. Ye, Q. Li and Z. Li, *Adv. Mater.*, 2024, **36**, e2407875.
31 T. Ye, L. Fei, X. Chen, Y. Yin and C. Wang, *ACS Appl. Mater. Interfaces*, 2023, **15**, 4623–4634.
32 H. Zhao, B. Fan, S. Hu, X. L. Liu and P. Xue, *Chemistry*, 2025, e202404195.
33 B. Xu, J. He, Y. Mu, Q. Zhu, S. Wu, Y. Wang, Y. Zhang, C. Jin, C. Lo, Z. Chi, A. Lien, S. Liu and J. Xu, *Chem. Sci.*, 2015, **6**, 3236–3241.
34 A. Huang, Q. Li and Z. Li, *Chin. J. Chem.*, 2022, **40**, 2356–2370.
35 F. Yang, X. Wu, H. Cui, S. Jiang, Z. Ou, S. Cai and G. Hong, *J. Am. Chem. Soc.*, 2022, **144**, 18406–18418.
36 J.-C. Zhang, C.-N. Xu, S. Kamimura, Y. Terasawa, H. Yamada and X. Wang, *Opt. Express*, 2013, **21**, 12976–12986.
37 J.-C. Zhang, Y.-Z. Long, X. Yan, X. Wang and F. Wang, *Chem. Mater.*, 2016, **28**, 4052–4057.
38 J. Ming, Y. Chen, H. Miao, Y. Fan, S. Wang, Z. Chen, Z. Guo, Z. Guo, L. Qi, X. Wang, B. Yun, P. Pei, H. He, H. Zhang, Y. Tang, D. Zhao, G. K.-L. Wong, J.-C. G. Bünzli and F. Zhang, *Nat. Photonics*, 2024, **18**, 1254–1262.
39 R. Schmidt, M. Ströbele, C. P. Romao, D. Enseling, T. Jüstel and H.-J. Meyer, *Dalton Trans.*, 2019, **48**, 14069–14076.
40 C. Xu, J. Huang, Y. Jiang, S. He, C. Zhang and K. Pu, *Nat. Biomed. Eng.*, 2023, **7**, 298–312.
41 W. Wang, K. W. Kevin Tang, I. Pyatnitskiy, X. Liu, X. Shi, D. Huo, J. Jeong, T. Wynn, A. Sangani, A. Baker, J.-C. Hsieh, A. R. Lozano, B. Artman, L. Fenno, V. P. Buch and H. Wang, *ACS Nano*, 2023, **17**, 24936–24946.
42 W. Wang, I. Pyatnitskiy, Y. Shi, K. W. K. Tang, Y. Xie, T. Wynn, X. Liu, J.-C. Hsieh, J. Jeong, W. He, B. Artman, A. R. Lozano, X. Shi, A. Sangani, L. Fenno, S. Santacruz, B. Chen and H. Wang, *bioRxiv*, 2025, preprint, DOI: 10.1101/2025.01.03.631271.
43 W. Wang, Y. Shi, W. Chai, K. W. K. Tang, I. Pyatnitskiy, Y. Xie, X. Liu, W. He, J. Jeong, J.-C. Hsieh, A. R. Lozano,

B. Artman, X. Shi, N. Hoefer, B. Shrestha, N. B. Stern, W. Zhou, D. W. McComb, T. Porter, G. Henkelman, B. Chen and H. Wang, *Nature*, 2025, **638**, 401–410.
44 Y. Wang, Z. Yi, J. Guo, S. Liao, Z. Li, S. Xu, B. Yin, Y. Liu, Y. Feng, Q. Rong, X. Liu, G. Song, X.-B. Zhang and W. Tan, *Nat. Photonics*, 2024, **18**, 334–343.
45 Z. Xie, H. Deng, X. Ge, Z. Chi and B. Liu, *J. Am. Chem. Soc.*, 2025, **147**(15), 12722–12729.
46 X. Pan, Y. Zhuang, W. He, C. Lin, L. Mei, C. Chen, H. Xue, Z. Sun, C. Wang, D. Peng, Y. Zheng, C. Pan, L. Wang and R.-J. Xie, *Nat. Commun.*, 2024, **15**, 2673.
47 W. Wang, Z. Wang, J. Zhang, J. Zhou, W. Dong and Y. Wang, *Nano Energy*, 2022, **94**, 106920.
48 J. M. Ha, S. H. Hur, A. Pathak, J.-E. Jeong and H. Y. Woo, *NPG Asia Mater.*, 2021, **13**, 53.
49 T. Schweizer, H. Kubach and T. Koch, *Automot. Engine Technol.*, 2021, **6**, 275–287.
50 A. Mateo-Alonso, *Chem. Mater.*, 2023, **35**, 1467–1469.
51 N. Zhang, X.-T. Wang, Z. Xiong, L.-Y. Huang, Y. Jin, A.-J. Wang, P.-X. Yuan, Y.-B. He and J.-J. Feng, *Anal. Chem.*, 2021, **93**, 17110–17118.
52 B. P. Chandra, V. K. Chandra, P. Jha, R. Patel, S. K. Shende, S. Thaker and R. N. Baghel, *J. Lumin.*, 2012, **132**, 2012–2022.
53 S. Jiang, X. Wu, F. Yang, N. J. Rommelfanger and G. Hong, *Nat. Protoc.*, 2023, **18**, 3787–3820.
54 G. Kim, V. M. Lau, A. J. Halmes, M. L. Oelze, J. S. Moore and K. C. Li, *Proc. Natl. Acad. Sci. U. S. A.*, 2019, **116**, 10214–10222.
55 P. Liu, Y.-L. Tseng, L. Ge, T. Zeng, D. Shabat and M. J. Robb, *J. Am. Chem. Soc.*, 2024, **146**, 22151–22156.
56 X. Xing, S. Zhao, T. Xu, L. Huang, Y. Zhang, M. Lan, C. Lin, X. Zheng and P. Wang, *Coord. Chem. Rev.*, 2021, **445**, 214087.
57 R. Wu, Z. Yao, Z. Chen, X. Ge, L. Su, S. Wang, Y. Wu and J. Song, *Anal. Chem.*, 2023, **95**, 11219–11226.
58 Y. Du, X. Liu and S. Zhu, *Front. Chem.*, 2021, **9**, 718709.
59 Z. Dang, X. Liu, Y. Du, Y. Wang, D. Zhou, Y. Zhang and S. Zhu, *Adv. Mater.*, 2023, **35**, e2306773.
60 S. Chang, K. Zhang, D. Peng, Y. Deng, C.-X. Shan and L. Dong, *Nano Energy*, 2024, **122**, 109325.
61 Z. Yao, F. Xu, R. Wu, X. Wang, M. Guo, S. Wang, K. Yang, W. Du and J. Song, *Anal. Chem.*, 2024, **96**, 15031–15041.
62 C. Patriarca, C. A. Clerici, S. Zannella and C. Fraticelli, *Pathologica*, 2021, **113**, 481–487.
63 R. F. Young, R. Kroening, W. Fulton, R. A. Feldman and I. Chambi, *J. Neurosurg.*, 1985, **62**, 389–396.
64 P. Boon, R. Raedt, V. de Herdt, T. Wyckhuys and K. Vonck, *Neurotherapeutics*, 2009, **6**, 218–227.
65 A. P. Yadav and M. A. L. Nicolelis, *Mov. Disord.*, 2017, **32**, 820–832.
66 E. M. Wassermann and T. Zimmermann, *Pharmacol. Ther.*, 2012, **133**, 98–107.
67 Y. Pan, C. Pan, L. Mao and P. Yu, *Fundam. Res.*, 2025, **5**, 55–62.
68 L. Cooper, M. G. Malinao and G. Hong, *Acc. Chem. Res.*, 2024, **57**, 1384–1397.
69 K. Deisseroth, G. Feng, A. K. Majewska, G. Miesenböck, A. Ting and M. J. Schnitzer, *J. Neurosci.*, 2006, **26**, 10380–10386.
70 H. Guo, M. Hamilton Ii, S. J. Offutt, C. D. Gloeckner, T. Li, Y. Kim, W. Legon, J. K. Alford and H. H. Lim, *Neuron*, 2018, **99**, 866.
71 T. Liu, M. H. Choi, J. Zhu, T. Zhu, J. Yang, N. Li, Z. Chen, Q. Xian, X. Hou, D. He, J. Guo, C. Fei, L. Sun and Z. Qiu, *Brain Stimul.*, 2022, **15**, 1308–1317.
72 C.-N. Xu, T. Watanabe, M. Akiyama and X.-G. Zheng, *Appl. Phys. Lett.*, 1999, **74**, 2414–2416.
73 F. Yang, S.-J. Kim, X. Wu, H. Cui, S. K. Hahn and G. Hong, *Adv. Drug Delivery Rev.*, 2023, **194**, 114711.
74 K. Deisseroth, *Nat. Neurosci.*, 2015, **18**, 1213–1225.
75 J. Yang, S. Zhao, J. Wang, S. Lin, Q. Hou and M. Sawan, *Front. Neurosci.*, 2024, **18**, 1340164.
76 L. K. Griffeth, *Proc. (Bayl. Univ. Med. Cent.)*, 2005, **18**, 321–330.
77 Z. Shaikh, A. Torres and M. Takeoka, *Brain Sci.*, 2019, **9**, 190.
78 G. Foti and C. Longo, *Pol. J. Radiol.*, 2024, **89**, e443–e451.
79 F. Reyes-Santias, C. García-García, B. Aibar-Guzmán, A. García-Campos, O. Cordova-Arevalo, M. Mendoza-Pintos, S. Cinza-Sanjurjo, M. Portela-Romero, P. Mazón-Ramos and J. R. Gonzalez-Juanatey, *Healthcare*, 2023, **11**, 2084.
80 L. Arms, D. W. Smith, J. Flynn, W. Palmer, A. Martin, A. Woldu and S. Hua, *Front. Pharmacol*, 2018, **9**, 802.
81 D. Le, D. Dhamecha, A. Gonsalves and J. U. Menon, *Front. Bioeng. Biotechnol.*, 2020, **8**, 25.
82 C. Xu, S. He, X. Wei, J. Huang, M. Xu and K. Pu, *Adv. Mater.*, 2023, **35**, e2211651.
83 D. B. Moyano, D. A. Paraiso and R. A. González-Lezcano, *Healthcare*, 2022, **10**, 423.
84 Z. Wang, Z. Feng, F. Du, X. Xiang, X. Tang, L. Qiu and Z. Qian, *Chin. Chem. Lett.*, 2023, **34**, 108137.
85 K. A. Michaelis, M. A. Norgard, X. Zhu, P. R. Levasseur, S. Sivagnanam, S. M. Liudahl, K. G. Burfeind, B. Olson, K. R. Pelz, D. M. Angeles Ramos, H. C. Maurer, K. P. Olive, L. M. Coussens, T. K. Morgan and D. L. Marks, *Nat. Commun.*, 2019, **10**, 4682.
86 W. Wu, L. Shi, Y. Duan, S. Xu, L. Shen, T. Zhu, L. Hou, X. Meng and B. Liu, *Biomaterials*, 2021, **274**, 120870.
87 Y. Tang, Y. Li, B. Li, W. Song, G. Qi, J. Tian, W. Huang, Q. Fan and B. Liu, *Nat. Commun.*, 2024, **15**, 2530.
88 P. Tan, L. He, Y. Huang and Y. Zhou, *Physiol. Rev.*, 2022, **102**, 1263–1325.
89 H. An, C. Yang, Z. Jiang, J. Yuan, Z. Qiu, L. Chen, X. Chen, M. Huang, L. Huang, H. Lin, B. Cheng, H. Liu and Z. Yu, *Chin. Chem. Lett.*, 2024, **35**, 109134.
90 X. Li, Z. Wang, J. He, H. Al-Mashriqi, J. Chen and H. Qiu, *Chem. Sci.*, 2024, **16**, 29–42.
91 Z. Yang, X. Shen, J. Jin, X. Jiang, W. Pan, C. Wu, D. Yu, P. Li, W. Feng and Y. Chen, *Adv. Sci.*, 2024, **11**, 2400251.
92 L. Qiu, Z. Zhu, J. Liang, X. Qiao, H. Xu, H. Xiang, H. Ding and Y. Chen, *Coord. Chem. Rev.*, 2024, **500**, 215531.
93 A. Massey, J. Stewart, C. Smith, C. Parvini, M. McCormick, K. Do and A. X. Cartagena-Rivera, *Nat. Rev. Phys.*, 2024, **6**, 269–282.